JCTC Journal of Chemical Theory and Computation

pubs.acs.org/JCTC Article

Simulating Periodic Systems on a Quantum Computer Using Molecular Orbitals

Jie Liu, Lingyun Wan, Zhenyu Li,* and Jinlong Yang*

Cite This: J. Chem. Theory Comput. 2020, 16, 6904−6914 Read Online

ACCESS | Metrics & More | Article Recommendations

ABSTRACT: The variational quantum eigensolver (VQE) is one of the most appealing quantum algorithms to simulate electronic structure properties of molecules on near-term noisy intermediate-scale quantum devices. In this work, we generalize the VQE algorithm for simulating periodic systems. However, the numerical study of a one-dimensional (1D) infinite hydrogen chain using existing VQE algorithms shows a remarkable deviation of the ground-state energy with respect to the exact full configuration interaction (FCI) result. Here, we present two schemes to improve the accuracy of quantum simulations for periodic systems. The first one is a modified VQE algorithm, which introduces a unitary transformation of Hartree−Fock orbitals to avoid the complex wave function. The second one is combining VQE with the quantum subspace expansion approach (VQE/QSE). Numerical benchmark calculations demonstrate that both of the two schemes provide an accurate description of the potential energy curve of the 1D hydrogen chain. In addition, excited states computed with the VQE/QSE approach also agree very well with FCI results.

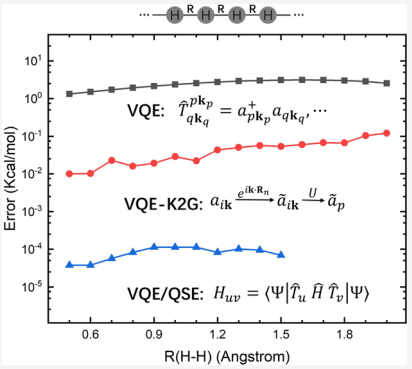

1. INTRODUCTION

A well-defined, accurate, and efficient electronic structure method is critical for interpreting material properties and for the prediction and designing of novel materials. Over the years, a huge amount of effort has been devoted to systematically improve the computational accuracy for material simulations. Density functional theory (DFT) is a very powerful and elegant first-principles method to explore ground-state properties of solids in materials science and condensed matter physics, while the accuracy of DFT calculations strongly depends on exchange-correlation functional approximations.[1−3] Recently, wave function based periodic electronic structure methods, such as second-order Møller−Plesset perturbation theory and coupled-cluster (CC) theory, have been successfully applied to problems in solids and low-dimensional nanomaterials.[4−11] Although wave function based methods offer a systematic approach for solving the many electron Schrödinger equation, their computational cost for accurately capturing strong electronic correlation effects is often prohibitive. For example, coupled-cluster theory with single and double excitations (CCSD) plus perturbative triples correction known as the gold standard in quantum chemistry[12] scales like the seventh power of the system size, while the exact full configuration interaction (FCI) approach scales exponentially.

The recent advent of quantum computing provides a new pathway for solving the many electron Schrödinger equation in polynomial time.[13−17] With rapid progress in quantum chemistry based quantum algorithms, experimental studies of molecular ground-state and excited-state properties have been extensively performed.[18−27] For example, Du et al. reported a quantum phase estimation (QPE) simulation of the ground-state energy of the hydrogen molecule using NMR.[18] Peruzzo et al. first proposed and realized the variational quantum eigensolver (VQE) algorithm on a photonic quantum processor for computing the ground-state energy of HeH^+.[19] Colless et al. used a superconducting-qubit-based processor to apply the quantum subspace expansion (QSE) approach to the H_2 molecule, extracting both ground and excited states without the need for additional minimization.[28] Quantum simulations have also been extended to theoretical studies of periodic model systems.[16,29−33]

The QPE[34] and VQE algorithms[19] are two leading quantum algorithms for solving electronic structure problems on a quantum computer. The standard QPE algorithm evolves in time a quantum state under the Hamiltonian $\hat{H}$ of interest, which offers an exponential speedup for determining the molecular spectra over classical methods. However, the practical implementation of QPE requires a large, error-corrected quantum computer, which is believed to be out of

Received: August 25, 2020
Published: October 19, 2020

https://dx.doi.org/10.1021/acs.jctc.0c00881
J. Chem. Theory Comput. 2020, 16, 6904−6914

reach in near-term quantum devices. On the other side, VQE provides an alternative quantum algorithm for near-term noisy intermediate-scale hardware, because it requires a much shorter coherence time and can be implemented with massive parallelization.[21]

VQE applies the Rayleigh-Ritz variational principle to optimize the parametrized wave function, which finally minimizes the total energy functional. The variational optimization procedure is a hybrid quantum-classical algorithm, that is, the evaluation of various physical properties in terms of the expectation value of operators, such as the energy and gradient, is performed on the quantum computer and the update of parameters is performed on the classical computer.[28,35−38] Given the wave function, the expectation value of operators is obtained by repeating the measurement many times and taking an average of measurement values. Integrated with the quantum computer, the state preparation and measurement of Pauli operators can be carried out in polynomial time. Therefore, it is possible to efficiently compute the energy or gradient on the quantum computer even when the wave function involves exponential configurations. Considering the superiority of VQE on near-term quantum devices, it has been widely used to solve various electronic structure problems.[16] However, the application of VQE to periodic chemical systems is still lacking.

In this work, we generalize the VQE algorithm to periodic systems. The wave function ansatzes used in this work include the unitary coupled cluster (UCC) ansztz[19,39] and the Adaptive Derivative-Assembled Pseudo-Trotter ansatz (ADAPT) recently proposed by Grimsley et al.[27] Based on the periodic boundary condition, Hartree−Fock (HF) orbitals at sampling k-points are defined in the complex space with a periodic phase. Given anti-Hermitian operators used in UCC and ADAPT-VQE, the coefficients of operators are assumed to be real in order to obtain a unitary transformation. Therefore, the complex wave function variationally optimized in the real parameter space converges to a local minimum as discussed later in this work. In order to overcome this problem, we propose a modified VQE algorithm, named the VQE-K2G approach, which converts HF orbitals at sampling k-points in a unit cell into real orbitals at Γ-point in the corresponding supercell. After that, the wave function and Hamiltonian are also defined in the real space. Therefore, VQE-K2G for periodic systems is expected to be as accurate as VQE for molecular systems. In addition, it is possible to improve the accuracy of VQE by combining it with QSE (VQE/QSE),[26] in which a reference state is prepared with VQE and the ground-state wave function is obtained by diagonalizing the Hamiltonian sampled on the linear-response space of the reference state. VQE/QSE is expected to offer a good estimation of the exact wave function if VQE can prepare a reasonable reference state.

This paper is organized as follows. Section 2 gives a brief description of the theoretical methodology, covering the periodic Hartree−Fock method, VQE algorithms with UCC and ADAPT ansatzes, the VQE algorithm for periodic systems, and the VQE/QSE approach. In section 3, we first compute the ground-state potential energy curve of an equispaced one-dimensional (1D) infinite hydrogen chain and analyze errors for different wave function ansatzes. We then assess the accuracy of two schemes, VQE-K2G and VQE/QSE, for ground-state calculations. Finally, we compute the potential energy curve of the first excited state for the 1D hydrogen chain with the VQE/QSE approach. A summary and outlook are given in Section 4.

2. THEORY

2.1. Periodic Hartree−Fock Method. For the periodic system using atom-centered basis sets, Bloch atomic orbitals (BAO) are defined as

$$\chi_{\mu\mathbf{k}}(\mathbf{r}) = \frac{1}{\sqrt{N}} \sum_{\mathbf{R}_n} e^{i\mathbf{k}\cdot\mathbf{R}_n} \chi_\mu(\mathbf{r} - \mathbf{R}_n) \tag{1}$$

where $\mathbf{R}_n$ is a translation vector, $\mathbf{k}$ is a crystal momentum vector sampled in the unit cell, and N is the number of unit cells. HF orbitals at $\mathbf{k}$ are expanded as a linear combination of BAOs

$$\phi_{p\mathbf{k}}(\mathbf{r}) = \sum_\mu C_{\mu p}(\mathbf{k}) \chi_{\mu\mathbf{k}}(\mathbf{r}) \tag{2}$$

which is also known as the Hartree−Fock−Roothaan approximation in first-principles molecular calculations. Given HF orbitals, the corresponding one- and two-electron integrals can be computed.[40] The core electron potential is represented with the norm-conserving HGH pseudopotential,[41−43] which removes the Coulomb singularity at the origin.

For each $\mathbf{k}$, the Hartree−Fock eigenvalue equation is expressed in the representation of BAOs as

$$F(\mathbf{k})C(\mathbf{k}) = S(\mathbf{k})C(\mathbf{k})E(\mathbf{k}) \tag{3}$$

The Fock and overlap matrix elements are given by

$$\begin{aligned} F_{\mu\nu}(\mathbf{k}) &= T_{\mu\nu}(\mathbf{k}) + V^{\mathrm{PP}}_{\mu\nu}(\mathbf{k}) + J_{\mu\nu}(\mathbf{k}) - K_{\mu\nu}(\mathbf{k}) \\ S_{\mu\nu}(\mathbf{k}) &= \int_\Omega \chi^*_{\mu\mathbf{k}}(\mathbf{r}) \chi_{\nu\mathbf{k}}(\mathbf{r}) d\mathbf{r} \end{aligned} \tag{4}$$

Here, $\mathbf{T}$ is the kinetic energy, $\mathbf{V}^{\mathrm{PP}}$ is the pseudopotential, $\mathbf{J}$ is the Coulomb integral, and $\mathbf{K}$ is the exchange integral. In the real space, these matrices are given by

$$\begin{aligned} T_{\mu\nu}(\mathbf{k}) &= -\frac{1}{2} \int_\Omega \chi^*_{\mu\mathbf{k}}(\mathbf{r}) \nabla^2_{\mathbf{r}} \chi_{\nu\mathbf{k}}(\mathbf{r}) d\mathbf{r} \\ J_{\mu\nu}(\mathbf{k}) &= \int\int_\Omega \chi_{\mu\mathbf{k}}(\mathbf{r}) \frac{\rho(\mathbf{r}', \mathbf{r}')}{|\mathbf{r} - \mathbf{r}'|} \chi^*_{\nu\mathbf{k}}(\mathbf{r}) d\mathbf{r} d\mathbf{r}' \\ K_{\mu\nu}(\mathbf{k}) &= \int\int_\Omega \chi_{\mu\mathbf{k}}(\mathbf{r}) \frac{\rho(\mathbf{r}, \mathbf{r}')}{|\mathbf{r} - \mathbf{r}'|} \chi^*_{\nu\mathbf{k}}(\mathbf{r}') d\mathbf{r} d\mathbf{r}' \end{aligned} \tag{5}$$

where Ω indicates that the real space integration is performed in the unit cell. The density matrix can be obtained by averaging over sampling k-points in a unit cell

$$\rho(\mathbf{r}, \mathbf{r}') = \frac{1}{N_\mathbf{k}} \sum_\mathbf{k} \sum_i^{N_o} \phi_{i\mathbf{k}}(\mathbf{r}) \phi^*_{i\mathbf{k}}(\mathbf{r}') \tag{6}$$

where N_k is the number of k-points, and N_o is the number of occupied electrons.

Note that we use atom-centered basis sets in this work, but the formulation presented here and after can be straightforwardly generalized to other basis sets, such as plane waves. The plane wave basis set is particularly suitable for periodic material simultions. Especially, as discussed in ref 29, the number of terms in the Hamiltonian with the plane wave and plane wave dual basis sets scale $O(M^3)$ and $O(M^2)$, respectively. However, the number of plane waves is often 2−3 magnitude larger than

https://dx.doi.org/10.1021/acs.jctc.0c00881
J. Chem. Theory Comput. 2020, 16, 6904−6914

that of atom-centered basis sets. The plane wave is therefore considered as a long-term method for quantum simulations of materials. An alternative approach on near-term quantum devices is to construct Wannier basis functions[44] from plane waves, which have been widely used in the correlated wave function methods for materials.

2.2. VQE Algorithm. In the VQE algorithm, one key ingredient is the wave function ansatz, which prepares an electronic state with a parametrized unitary operator[36]

$$|\psi(\vec{\theta})\rangle = U(\vec{\theta})|\psi_0\rangle \tag{7}$$

where $|\psi_0\rangle$ is the reference state. The parametrized wave function is optimized through the Rayleigh-Ritz variational principle

$$E_0 = \min_{\vec{\theta}}\{\langle\psi(\vec{\theta})|\hat{H}|\psi(\vec{\theta})\rangle\} \tag{8}$$

The Hamiltonian in the second-quantized representation is expressed as

$$\hat{H} = \sum_{pq} h_q^p \hat{T}_q^p + \frac{1}{2}\sum_{pqrs} h_{rs}^{pq}\hat{T}_{rs}^{pq} \tag{9}$$

where h_q^p is the one-electron integral, including kinetic energy and ionic potential (pseudopotential in this work), and h_{rs}^{pq} is the two-electron integral

$$h_{rs}^{pq} = \int\int \phi_p^*(\mathbf{r}_1)\phi_q^*(\mathbf{r}_2)\frac{1}{|\mathbf{r}_1 - \mathbf{r}_2|}\phi_r(\mathbf{r}_2)\phi_s(\mathbf{r}_1)d\mathbf{r}_1 d\mathbf{r}_2 \tag{10}$$

The general one- and two-body operators are defined as[45,46]

$$\hat{T}_q^p = \hat{a}_p^\dagger \hat{a}_q$$
$$\hat{T}_{rs}^{pq} = \hat{a}_p^\dagger \hat{a}_q^\dagger \hat{a}_r \hat{a}_s \tag{11}$$

where $a_p^\dagger$ and a_p are the second-quantized creation and annihilation operators, satisfying the anticommutation relation.

2.2.1. Unitary Coupled Cluster Ansatz. The unitary CC (UCC) ansatz is a common component in quantum variational algorithms.[39,47−50] Different from the traditional CC (tCC) theory, the UCC energy and wave function are variationally determined according to eq 8. The UCC wave function is defined as

$$|\psi\rangle = e^{T-T^\dagger}|\psi_0\rangle \tag{12}$$

A cluster operator for unitary CCSD (UCCSD) is expressed as[49]

$$\hat{T} = \sum_{ai} t_i^a \hat{T}_i^a + \frac{1}{4}\sum_{abij} t_{ij}^{ab}\hat{T}_{ij}^{ab} \tag{13}$$

Recently, a cluster operator for UCC with *generalized* one- and two-body operators (UCCGSD) has been introduced in the VQE algorithm[19,46,51−53]

$$\hat{T} = \frac{1}{2}\sum_{pq} t_q^p \hat{T}_q^p + \frac{1}{4}\sum_{pqrs} t_{rs}^{pq}\hat{T}_{rs}^{pq} \tag{14}$$

Here, *a*, *b*, ... indicate virtual orbitals; *i*, *j*, ... indicate occupied orbitals; and *p*, *q*, ... indicate general orbitals.

Although UCC is more robust than tCC, neither UCCSD nor UCCGSD can be expanded using the Baker−Campbell−Hausdorff (BCH) formula at finite order. Therefore, an exact implementation of UCC on a classical computer scales exponentially. However, the UCC wave function can be easily prepared on a quantum computer even if the reference state is a multiconfigurational state. Recently, the UCC ansatz has been successfully used in experimental and theoretical quantum simulations of chemical systems with the VQE algorithm.[19,54]

At convergence, the stationary of the energy with respect to parameters is expressed as

$$\frac{\partial\langle\psi(\vec{t})|\hat{H}|\psi(\vec{t})\rangle}{\partial t_u} = 0 \tag{15}$$

where t_u is the coefficient of anti-Hermitian operators $\tau_u \in \{\hat{T}_q^p - \hat{T}_p^q, \hat{T}_{rs}^{pq} - \hat{T}_{qp}^{sr}\}$ for UCCGSD and $\tau_u \in \{\hat{T}_i^a - \hat{T}_a^i, \hat{T}_{ij}^{ab} - \hat{T}_{ba}^{ij}\}$ for UCCSD. Recent numerical studies of small molecules with minimum basis sets demonstrate UCCGSD is far more robust and accurate than UCCSD.[55] The difference between UCCSD and UCCGSD is even more significant for periodic numerical simulations as shown later in this work.

On quantum computers, the implementation of UCC requires a decomposition of the exponentiated cluster operator into one- and two-qubit gates using an approximate scheme, such as the Trotter−Suzuki decomposition[56−58]

$$e^{\hat{A}+\hat{B}} \approx (e^{\hat{A}/k}e^{\hat{B}/k})^k \tag{16}$$

The UCC wave function with Trotterization is defined as

$$|\psi\rangle = \lim_{N\to\infty}\prod_{k=1}^{N}\prod_{u}^{N_u} e^{\frac{t_u}{N}\tau_u}|\psi_0\rangle \tag{17}$$

Therefore, the accuracy of UCC-VQE simulations strongly depends on the Trotter formula used, the number of Trotter steps, and the time-ordered sequence of operators in the UCC ansatz. In principle, a low-order Trotter−Suzuki decomposition probably results in a large error. However, given the wave function expression in eq 17, the optimization of the wave function in the parameter space is able to cancel part of the error and give a promising estimation of the ground-state energy.

2.2.2. ADAPT Ansatz. Grimsley et al. recently proposed to approximate the exact wave function as an arbitrarily long product of general one- and two-body exponentiated operators[27]

$$|\psi(\vec{\theta})\rangle = \lim_{N\to\infty}\prod_{k=1}^{N}\prod_{u}^{N_u} e^{\theta_u(k)\tau_u}|\psi_0\rangle \tag{18}$$

In order to generate a maximally compact sequence of operators at convergence, the operator, $\tau(k)$, with the largest absolute *pre-estimated* gradient instead of all operators in the operator pool O is used to update the wave function ansatz in the k-th iteration. This indicates $N_u = 1$ in eq 18. The wave function is iteratively updated with

$$|\psi(k)\rangle = e^{\theta(k)\tau(k)}|\psi(k-1)\rangle \tag{19}$$

where $|\psi(0)\rangle = |\psi_0\rangle$ is the reference state. The energy functional in the k-th iteration is minimized by

$$E(k) = \min_{\{\theta(l)\}_{l=1}^{k}}\{\langle\psi(k)|\hat{H}|\psi(k)\rangle\} \tag{20}$$

The gradient of the energy functional with respect to parameters $\{\theta(l)\}_{l=1}^{k}$ is formulated as

https://dx.doi.org/10.1021/acs.jctc.0c00881
J. Chem. Theory Comput. 2020, 16, 6904−6914

$$G_l = \frac{\partial E(k)}{\partial \theta(l)} = 2\Re\left(\langle\psi(k)|\hat{H}\prod_{m=l+1}^{k}(e^{\theta(m)\tau(m)})\tau(l)\prod_{n=1}^{l}(e^{\theta(n)\tau(n)})|\psi_0\rangle\right) \quad (21)$$

The convergence criteria is defined as

$$|\vec{R}|_2 = \sqrt{\sum_u |R_u|^2} < \epsilon \quad (22)$$

where R_u is the *pre-estimated* gradient for the following iteration. For example, in the $(k+1)$-th iteration, R_u is defined with the wave function optimized in the k-th iteration

$$R_u = G_{k+1}|_{\theta_{k+1}=0,\tau(k+1)=\tau_u} = \langle\psi(k)|[\hat{H}, \tau_u]|\psi(k)\rangle \quad (23)$$

The variational optimization procedure for the ADAPT-VQE algorithm is summarized in Algorithm 1.

Algorithm 1 The ADAPT-VQE algorithm for optimizing the wave function and the energy.

Input: Reference state $|\psi_0\rangle$ and Hamiltonian $\hat{H}$.
Output: The energy and wave function of the target state.

1: Prepare the initial wave function $|\Psi\rangle = |\psi_0\rangle$ in qubit representation.
2: Define the operator pool $\mathcal{O}$.
3: Initialize the operator set $\vec{\tau} = \{\}$ and parameters $\vec{\theta} = \{0\}$.
4: **while** $|\vec{R}|_2 > \epsilon$ **do**
5: Compute $\{\vec{R}\}$ with Eq. (23) for all $\tau_u \in \mathcal{O}$.
6: $\vec{\tau} \leftarrow \{\vec{\tau}, \tau_u\}$ with $|R_u|$ being the largest absolute *pre-estimated* gradient and $\vec{\theta} = \{\vec{\theta}, 0\}$.
7: Define the new wave function with Eq.(19) and the new energy functional with Eq. (20).
8: Optimize parameters $\vec{\theta}$.
9: **end while**
10: Return $E(\vec{\theta})$ and $|\psi(\vec{\theta})\rangle$.

2.3. VQE Algorithm for Periodic Systems. To extend VQE algorithms for periodic systems, we define the general one- and two-body operator pool with Hartree−Fock orbitals of eq 2[53,59,60]

$$\hat{T}_{\tilde{r}}^{\tilde{p}} = \hat{a}_{\tilde{p}}^{\dagger}\hat{a}_{\tilde{r}}$$
$$\hat{T}_{\tilde{r}\tilde{s}}^{\tilde{p}\tilde{q}} = \hat{a}_{\tilde{p}}^{\dagger}\hat{a}_{\tilde{q}}^{\dagger}\hat{a}_{\tilde{r}}\hat{a}_{\tilde{s}} \quad (24)$$

where $\tilde{p} = p\mathbf{k}_p$. The Hamiltonian is summed over sampling k-points in a unit cell

$$\hat{H} = \sum_{\tilde{p}\tilde{r}}{}' h_{\tilde{r}}^{\tilde{p}}\hat{T}_{\tilde{r}}^{\tilde{p}} + \frac{1}{2}\sum_{\tilde{p}\tilde{q}\tilde{r}\tilde{s}}{}' h_{\tilde{r}\tilde{s}}^{\tilde{p}\tilde{q}}\hat{T}_{\tilde{r}\tilde{s}}^{\tilde{p}\tilde{q}} \quad (25)$$

Because the Hamiltonian satisfies the translational symmetry based on the periodic boundary condition, general one- and two-body operators must conserve crystal momentum

$$\sum_{\tilde{p}}\mathbf{k}_{\tilde{p}} - \sum_{\tilde{r}}\mathbf{k}_{\tilde{r}} = \mathbf{G}_m \quad (26)$$

where $\mathbf{k}_{\tilde{p}}$ and $\mathbf{k}_{\tilde{r}}$ are crystal momenta of creation operators and annihilation operators, respectively. $\mathbf{G}_m$ is a reciprocal lattice vector. The primed summation in eq 25 indicates that one of the orbital momenta is fixed according to eq 26.

In order to analyze the difference of VQE based on real and complex HF orbitals, we first introduce the contracted Schrödinger equation (CSE), which can be derived by contraction of the Schrödinger equation onto the space of two particles

$$\langle\psi|\hat{T}_u\hat{H}|\psi\rangle = E\langle\psi|\hat{T}_u|\psi\rangle \quad (27)$$

Here, $\hat{T}_u \in \{\hat{T}_q^p, \hat{T}_{rs}^{pq}\}$. The anti-Hermitian CSE (ACSE) is expressed as

$$\langle\psi|[\hat{T}_u, \hat{H}]|\psi\rangle = 0 \quad (28)$$

which is also known as the Brillouin condition.[61,62] The ACSE can be written as a sum of the real part (ACSE-Re)

$$\langle\psi|[\hat{T}_u - \hat{T}_u^{\dagger}, \hat{H}]|\psi\rangle = 0 \quad (29)$$

and the imaginary part (ACSE-Im)

$$\langle\psi|[\hat{T}_u + \hat{T}_u^{\dagger}, \hat{H}]|\psi\rangle = 0 \quad (30)$$

For the real wave function, eq 29 is equivalent to the convergence criteria of ADAPT-VQE as shown in eq 22, and eq 30 is automatically satisfied since the wave function is real. Therefore, the variationally optimized ADAPT-VQE wave function is exactly the solution of eq 28. This agrees with the conclusion that the ACSE enforce stationary of the energy with respect to a sequence of unitary transformation of the reference state. As the Bloch wave function is introduced, eq 29 is still satisfied due to the variational optimization procedure, while the residual error of ACSE-Im that results in the deviation of the energy is not guaranteed to be minimized. In order to remove the residual error of ACSE-Im, we transform HF orbitals at sampling k-points in a unit cell into orbitals at Γ-point in the corresponding supercell. This generates a set of real wave function and Hamiltonian for the VQE algorithm. A brief introduction of this scheme, named K2G, is described as follows. HF orbitals in eq 2 can be rewritten as

$$\phi_{i\mathbf{k}}(\mathbf{r}) = \sum_{\tilde{\mu}}\tilde{C}_{\tilde{\mu}i\mathbf{k}}\chi_{\tilde{\mu}}(\mathbf{r}) \quad (31)$$

where

$$\tilde{C}_{\tilde{\mu}i\mathbf{k}} = \frac{1}{\sqrt{N}}e^{i\mathbf{k}\cdot\mathbf{R}_n}C_{\mu i}(\mathbf{k}) \quad (32)$$

and $\tilde{\mu}$ is the μ-th atomic orbital in the n-th "replica".

The eigenvalue equation for the supercell is formulated as

$$\sum_{\tilde{\nu}}F_{\tilde{\mu}\tilde{\nu}}^{sc}C_{\tilde{\nu}p} = \varepsilon_{\tilde{p}}\sum_{\tilde{\nu}}S_{\tilde{\mu}\tilde{\nu}}^{sc}C_{\tilde{\nu}p} \quad (33)$$

where $\mathbf{F}^{sc}$ and $\mathbf{S}^{sc}$ are the Fock and overlap matrices for the supercell. A detailed derivation of eq 33 is given in the Appendix. Because the supercell Fock matrix is a unique and real matrix, the real supercell Hartree−Fock orbitals and orbital energies are obtained by solving eq 33.

2.4. Quantum Subspace Expansion. The quantum subspace expansion approach has experimentally and theoretically proven to be one of the most useful techniques on near-term noisy intermediate-scale quantum devices.[26,28,37,63] In the original implementation of QSE, the reference state is prepared with the UCCSD ansatz, and excited states are obtained by diagonalizing the Hamiltonian sampled on the linear response space with single excitations.[37] It is straightforward to include higher-order excitation operators in QSE but at the expense of a sharp increase of measurements.

Given a set of linear-response excitation operators, $\{\hat{T}_u\}$, the configuration state space is defined with the (general) one- and two-body operators of eq 24 as

$$|\psi_u\rangle = \hat{T}_u|\psi\rangle \quad (34)$$

https://dx.doi.org/10.1021/acs.jctc.0c00881
J. Chem. Theory Comput. 2020, 16, 6904−6914

The QSE wave function can be expressed as a linear combination of configuration state functions

$$|\psi^{\mathrm{QSE}}\rangle = \sum_u C_u |\psi_u\rangle \tag{35}$$

The energy and wave function of the ground and excited states can be obtained by solving a generalized eigenvalue problem in the configuration state space

$$\mathbf{H}^{\mathrm{QSE}}\mathbf{C} = \mathbf{S}^{\mathrm{QSE}}\mathbf{C}\mathbf{E} \tag{36}$$

with eigenvectors $\mathbf{C}$ and a diagonal matrix of eigenvalues $\mathbf{E}$. Here, the coefficients $\mathbf{C}$ are complex. The Hamiltonian matrix elements projected onto the configuration state space are given by

$$H_{u,v}^{\mathrm{QSE}} = \langle\psi|\hat{T}_u^\dagger \hat{H} \hat{T}_v|\psi\rangle \tag{37}$$

The overlap matrix elements are given by

$$S_{u,v}^{\mathrm{QSE}} = \langle\psi|\hat{T}_u^\dagger \hat{T}_v|\psi\rangle \tag{38}$$

which is required because the configuration states are not necessarily orthogonal to each other.

The QSE approach is kind of inspired by the linear response method. Unlike the K2G approach, the QSE wave function is not necessarily the accurate solution of the ACSE except that all configuration states are included in the linear response space. However, when a well-defined reference state is used or high-order operators are included, the QSE wave function is able to provide a very good approximation to the FCI wave function, which implies a quite small residual error of the ACSE. The inclusion of high-order excitations indicates a polynomially increasing computational cost, which is prohibitive in medium- and large-size calculations. The VQE algorithm, especially ADAPT-VQE, is able to efficiently generate a reasonable reference state to approximate the target state even starting from a single-configurational Hartree−Fock state. Here, we combine VQE with the QSE approach by truncating excitation operators up to second order and apply it to study the ground state and excited states.

3. RESULTS

All calculations are performed with the modified ADAPT-VQE code,[64] which uses OpenFermion[65] for mapping Fermion operators onto qubit operators and PYSCF[66] for all one- and two-electron integrals. The energy and wave function are optimized with the Broyden−Fletcher−Goldfarb−Shannon (BFGS) algorithm implemented in SciPy.[67] Gradients are computed with the finite difference approach for UCC-VQE and the analytical approach of eq 21 for ADAPT-VQE. All UCC-VQE calculations are performed without Trotterization, that is, eq 12 is used in our classical numerical simulations. All full configuration interaction results used for benchmark are obtained through explicitly diagonalizing the Hamiltonian in *Hilbert* space of qubits. The operator pool is composed of the spin-adapted operators in order to avoid the spin contamination. The SVZ basis set together with GTH pseudopotential is used for all calculations.

Hereafter, for simplicity, we use ADAPT(m) to indicate an ADAPT-VQE calculation with $\epsilon = 10^{-m}$ defined in eq 22. The prefix Γ indicates a calculation with HF orbitals at Γ-point in the supercell. For example, Γ-ADAPT(m) indicates an ADAPT(m) calculation using the K2G scheme. ADAPT-SD and QSE-SD indicate that only one- and two-body excitations from occupied orbitals to virtual orbitals are involved in ADAPT and QSE, respectively. As stated in eq 18, we can specify $N_u > 1$ in ADAPT-VQE calculations. In this work, we update the wave function using 30 operators identified with the largest absolute *pre-estimated* gradients in each iteration.

A 1D hydrogen chain with each hydrogen atom equispaced along a line is an interesting model system to explore elemental physical phenomena in modern condensed matter physics, such as an antiferromagnetic Mott phase and an insulator-to-metal transition.[68−71] It also bridges the gap between the simply Hubbard model and realistic bulk materials. Depending on different electronic spin alignments, the hydrogen chain can be a paramagnetic, antiferromagnetic, or ferromagnetic phase. In this work, we place two hydrogen atoms in a unit cell, which is the minimum model system used to study the magnetic properties. Here, we benchmark the VQE algorithm for this 1D hydrogen chain model with one- and two-electron integrals obtained from a closed-shell Hartree−Fock calculation, which generates a paramagnetic state. We vary the hydrogen−hydrogen bond length, R(H−H), and compute the potential energy curve of the hydrogen chain with various wave function ansatzes. In addition, we notice that a larger basis set and k-points sampling are required to accurately describe a periodic system. However, the performance of various wave function ansatzes is assessed with respect to the FCI result computed with the same basis set and k-points. This will be not significantly affected by the accuracy of the theoretical method. In the following, all calculations are performed with $1 \times 1 \times 4$ k-points, in which four k-points are sampled along the hydrogen chain and one k-point is sampled along two other orthogonal directions. In the VQE-K2G approach, the corresponding supercell atomic basis functions are obtained by including eight hydrogen atoms in this supercell.

3.1. Accuracy of VQE Algorithms. In Figure 1, we study the ground-state potential energy curve and the absolute energy error with HF, UCCSD-VQE, UCCGSD-VQE, ADAPT(3)-SD, ADAPT(3), and FCI by varying R(H−H). HF fails to reproduce the exact energy curve with the mean error (ME) of 32.37 kcal/mol, because the correlation effect totally misses in HF. UCCSD-VQE performs much better than HF with ME of 20.0 kcal/mol but still significantly deviates from the exact FCI result. UCCSD is able to treat most weakly correlated systems, while it suffers from the well-known problem of describing the strong electronic correlation effect. For example, as R(H−H) increases from 0.5 to 2.0 Å, the absolute energy error of UCCSD-VQE increases from 7.19 to 38.16 kcal/mol. Note that the error of UCCSD-VQE in calculations of the 1D hydrogen chain is much larger than those in molecular calculations. For example, the largest absolute energy error is only 9.19 kcal/mol in calculations of a challenging system N_2 with the STO-3G basis set.[55] ADAPT-SD shares the same operator pool with UCCSD. Here, ADAPT(3)-SD produces almost exactly the same result as UCCSD-VQE with the comparable ME of 19.87 kcal/mol. However, it should be kept in mind that ADAPT-SD and UCCSD are two different wave function ansatzes as discussed later.

UCCGSD-VQE gives a more promising ground-state potential curve with the ME of only 1.58 kcal/mol. This agrees with the conclusion revealed in the previous study that the UCCGSD ansatz is far more robust and accurate than the simple UCCSD ansatz.[55] Analogous to ADAPT(3)-SD and UCCSD-VQE, ADAPT(3) and UCCGSD-VQE also share the

https://dx.doi.org/10.1021/acs.jctc.0c00881
J. Chem. Theory Comput. 2020, 16, 6904−6914

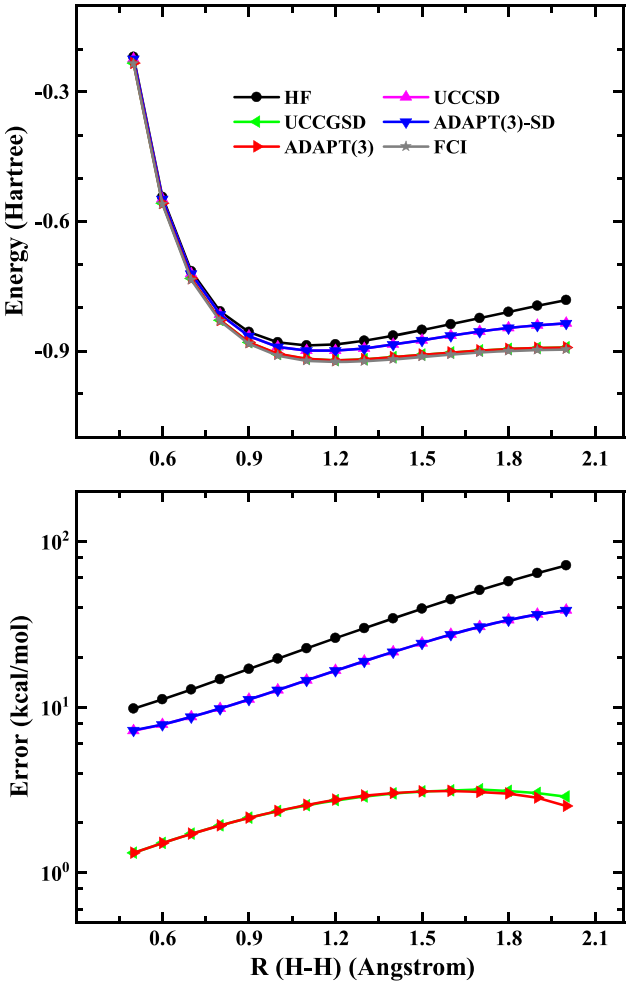

Figure 1. Ground-state potential energy curve and absolute energy error with respect to the FCI result for the 1D hydrogen chain computed with UCC-VQE and ADAPT-VQE using HF orbitals at sampling *k*-points.

same operator pool and give quite close results. However, ADAPT-VQE requires much fewer parameters to achieve the accuracy of UCCGSD-VQE. This is mainly because ADAPT-VQE approximates the exact wave function with a compact sequence of unitary transformation acting on the reference state. For example, the number of parameters in UCCGSD-VQE is fixed to be 236, while ADAPT(3) requires at most 144 parameters with R(H−H) varying from 0.5 to 2.0 Å. This is achieved at the cost of computing *pre-estimated* gradients in eq 23.

In addition, for ADAPT(3), the absolute energy error of the 1D hydrogen chain is 2−3 magnitude larger than those of small molecules (LiH, BeH_2, and H_6) presented in ref 27. As discussed in Section 2.3, these large deviations of the energy result from the complex wave function and Hamiltonian used in the VQE algorithm. In order to analyze errors in detail, Table 1 shows the maximum absolute residual error (MARE) of ACSE-Re and ACSE-Im for HF, UCCSD-VQE, UCCGSD-VQE, and ADAPT(3). MAREs of ACSE-Im in UCCGSD-VQE and ADAPT(3) are very close to those in HF and UCCSD-VQE, while MEs of the energy in UCCGSD-VQE and ADAPT(3) are much smaller than those in HF and UCCSD-VQE. This reveals that a majority of the absolute energy error in HF and UCCSD-VQE originate from larger residual errors of ACSE-Re. In UCCGSD-VQE and ADAPT(3), the variational algorithm efficiently minimizes the MARE of ACSE-Re (<0.1 kcal/mol), while it is not able to simultaneously minimize the MARE of ACSE-Im, which is left to be as large as ∼5.2 kcal/mol. Therefore, the error of UCCGSD-VQE and ADAPT(3) is largely attributed to the MARE of ACSE-Im. In order to improve the accuracy of the quantum variational algorithm for periodic systems, it is necessary to remove the residual error of ACSE-Im (see Table 2).

3.2. VQE-K2G Approach. In Figure 2(a), we show the absolute energy error of various VQE-K2G approaches as a function of R(H−H), which systematically remove the residual error of ACSE-Im through a unitary transformation of HF

Table 1. Maximum Absolute Residual Error (MARE) (in kcal/mol) of ACSE-Re and ACSE-Im for HF, UCCSD-VQE, UCCGSD-VQE, and ADAPT(3)[a]

	HF		UCCSD-VQE		UCCGSD-VQE		ADAPT(3)	
R	ACSE-Re	ACSE-Im	ACSE-Re	ACSE-Im	ACSE-Re	ACSE-Im	ACSE-Re	ACSE-Im
0.5	19.23	4.82	18.69	5.03	0.02	8.28	0.02	8.21
0.6	16.64	4.66	16.01	5.08	0.03	7.11	0.02	7.12
0.7	14.86	4.78	14.10	5.46	0.03	6.39	0.02	6.38
0.8	13.61	4.89	12.71	5.67	0.02	5.89	0.03	5.89
0.9	12.70	4.99	11.66	5.86	0.02	5.58	0.06	5.60
1.0	12.04	5.07	10.92	6.04	0.03	5.35	0.04	5.38
1.1	11.56	5.14	10.97	6.25	0.03	5.15	0.09	5.21
1.2	11.21	5.20	11.06	6.45	0.03	4.96	0.05	4.99
1.3	10.96	5.25	11.16	6.65	0.03	4.76	0.06	4.79
1.4	10.80	5.28	11.23	6.85	0.05	4.62	0.05	4.63
1.5	10.67	5.32	11.22	7.05	0.05	4.44	0.05	4.44
1.6	10.65	5.33	11.07	7.25	0.09	4.30	0.07	4.30
1.7	10.81	5.35	10.72	7.45	0.14	4.10	0.05	4.14
1.8	11.03	5.35	10.08	7.62	0.18	4.02	0.06	4.00
1.9	11.24	5.34	9.14	7.73	0.25	3.85	0.08	3.83
2.0	11.47	5.33	7.93	8.35	0.13	3.50	0.04	3.82
mMARE	12.47	5.13	11.79	6.55	0.09	5.16	0.05	5.17

[a]mMARE indicates the mean MARE.

https://dx.doi.org/10.1021/acs.jctc.0c00881
J. Chem. Theory Comput. 2020, 16, 6904−6914

Table 2. Mean Error (ME) of the Ground-State Energy (in kcal/mol) for Various Variational Approaches

	HF	UCCSD-VQE	UCCGSD-VQE	ADAPT(3)-SD	ADAPT(1)
ME	32.73	20.00	2.53	19.87	3.94
	ADAPT(2)	ADAPT(3)	Γ-UCCSD-VQE	Γ-ADAPT(3)-SD	Γ-ADAPT(X)-SD
ME	2.63	2.94	1.69	1.20	0.07
	Γ-ADAPT(3)	ADAPT(3)-SD/QSE-SD	ADAPT(3)-SD/QSE	ADAPT(1)/QSE	ADAPT(2)/QSE
ME	0.05	3.75	1.30	0.00	0.00

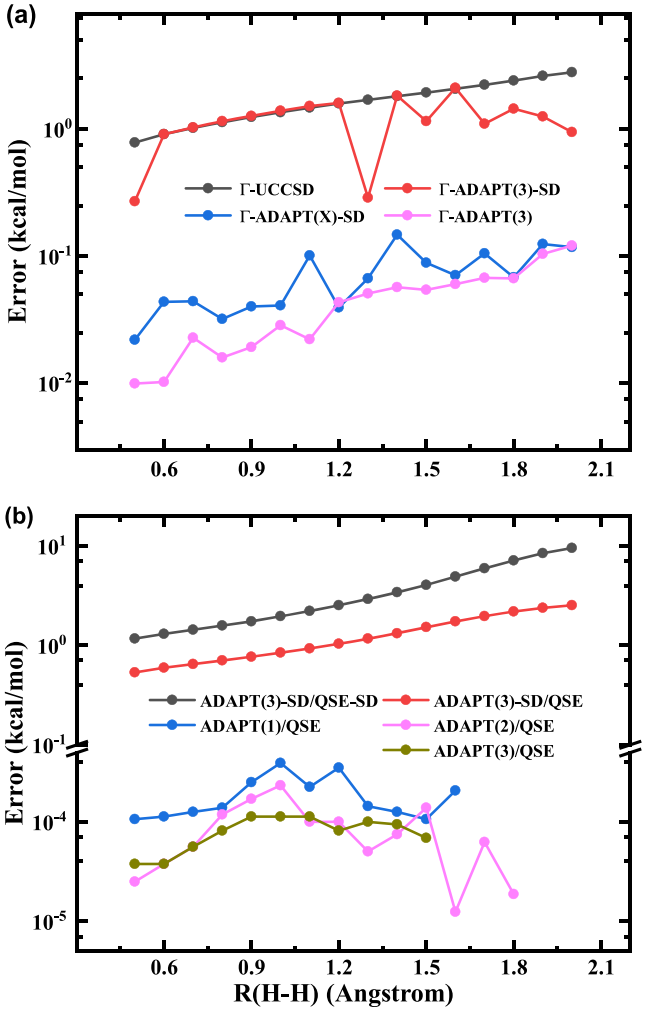

Figure 2. Error in the absolute energy of the VQE-K2G approach (a) and the VQE/QSE approach (b) for the ground state of the 1D hydrogen chain. Γ-ADAPT(X)-SD indicates $\epsilon = 2 \times 10^{-4}$. Vanishing points indicate zero error when the energies are recorded with eight decimal places in Hartree.

orbitals at sampling *k*-points. Analogous to molecular simulations, the potential energy curve computed with Γ-ADAPT(3) agrees quite well with the exact curve since the variationally optimized wave function strictly satisfies ACSE with the norm of residual errors less than 1×10^{-3}. ADAPT-VQE is an adaptive algorithm, and the wave function ansatz is self-consistently grown. Therefore, when the potential energy curve is scanned, the energy discontinuity may appear if the convergence thresh is not small enough. For example, errors in the absolute energy computed with Γ-ADAPT(3)-SD dramatically fluctuate as shown in Figure 2(a). Here, we also compute the energy with a tighter convergence thresh $\epsilon = 2 \times 10^{-4}$ in Γ-ADAPT(m)-SD, named Γ-ADAPT(X)-SD, for comparison. Γ-ADAPT(X)-SD gives well converged results with an ME of 0.07 kcal/mol, which is even comparable to ME of 0.05 kcal/mol in Γ-ADAPT(3).

In comparison with UCCSD-VQE, Γ-UCCSD-VQE gives a much better description of the potential energy curve of the 1D hydrogen chain. The maximum deviation of the energy for Γ-UCCSD-VQE at $R = 2.0$ Å is only 2.75 kcal/mol. Different from what is shown in Figure 1, Γ-ADAPT(3)-SD and Γ-ADAPT(X)-SD give more accurate results than Γ-UCCSD-VQE. In the ADAPT-VQE method, high-order excitations are ultimately included after a sequence of low-order exponentiated excitation operators acting on the wave function. A tighter convergence thresh implies that a larger N_k in eq 18 is required to converge the wave function ansatz. As N_k increases, the ADAPT-VQE wave function is, in principle, expanded in a larger configuration state space, which will improve the accuracy of the wave function ansatz. Therefore, the absolute energy error of Γ-ADAPT(m)-SD is reduced as *m* increases. This is very similar to the *k*-UpCCGSD approach, in which a larger *k* was often used to improve the accuracy.[55] UCCSD truncates excitation operators up to the second order, and its wave function is optimized in a fixed parameter space. The inclusion of higher-order excitation operators is the most straightforward way to improve the accuracy of Γ-UCCSD while at a steeply increasing computational cost.

It is worthy to mention that the accuracy of ADAPT(m)-SD cannot keep improving by increasing *m*. One important reason is the limitation of crystal momentum conservation in excitation operators when HF orbitals at sampling *k*-points are used. Given excitation operators in eq 24, it is impossible to generate these high-order excitations from the product of low-order excitation operators with crystal momentum conservation. For example, a quadruple excitation operator

$$\hat{T}^{\tilde{a}_1\tilde{a}_2\tilde{a}_3\tilde{a}_4}_{\tilde{i}_1\tilde{i}_2\tilde{i}_3\tilde{i}_4} = a^\dagger_{\tilde{a}_1} a^\dagger_{\tilde{a}_2} a^\dagger_{\tilde{a}_3} a^\dagger_{\tilde{a}_4} a_{\tilde{i}_1} a_{\tilde{i}_2} a_{\tilde{i}_3} a_{\tilde{i}_4} \tag{39}$$

conserves crystal momentum

$$\sum_{i=1}^{4} \mathbf{k}_{\tilde{a}_i} - \sum_{j=1}^{4} \mathbf{k}_{\tilde{i}_j} = \mathbf{G}_m \tag{40}$$

The quadruple excitation operator can be rewritten as

$$\hat{T}^{\tilde{a}_1\tilde{a}_2\tilde{a}_3\tilde{a}_4}_{\tilde{i}_1\tilde{i}_2\tilde{i}_3\tilde{i}_4} = \hat{T}^{\tilde{a}_1\tilde{a}_2}_{\tilde{i}_1\tilde{i}_2} \hat{T}^{\tilde{a}_3\tilde{a}_4}_{\tilde{i}_3\tilde{i}_4} \tag{41}$$

As a result, we reformulate the crystal momentum conservation of eq 40 as

$$\mathbf{k}_{\tilde{a}_1} + \mathbf{k}_{\tilde{a}_2} - \mathbf{k}_{\tilde{i}_1} - \mathbf{k}_{\tilde{i}_2} = -(\mathbf{k}_{\tilde{a}_3} + \mathbf{k}_{\tilde{a}_4} - \mathbf{k}_{\tilde{i}_3} - \mathbf{k}_{\tilde{i}_4}) + \mathbf{G}_m \tag{42}$$

which indicates that eq 26 is only a sufficient but not necessary condition of eq 40. Therefore, ADAPT(m)-SD optimizes the wave function in a limited subspace of configuration states, which can not be simply overcome by increasing *m*. Analogous

https://dx.doi.org/10.1021/acs.jctc.0c00881
J. Chem. Theory Comput. 2020, 16, 6904−6914

to UCCSD, the explicit inclusion of higher-order excitations is necessary to improve the accuracy of ADAPT-SD.

3.3. Quantum Subspace Expansion. The quantum subspace expansion approach is a robust quantum algorithm to improve the estimation of the energy over the reference state. On the other hand, the VQE/QSE approach that employs the VQE wave function as the reference state is expected to be able to provide complementary insights of various VQE schemes using Hartree−Fock orbitals at *k*-points. In Figure 2(b), we present the absolute energy error of the VQE/QSE approach as a function of R(H−H). Here, the reference states are prepared with ADAPT(3)-SD, ADAPT(1), ADAPT(2), and ADAPT(3). The Hamiltonian matrix elements are sampled in the linear-response space of the VQE wave function with (general) one- and two-body operators.

All energy curves computed with ADAPT(m)/QSE exactly reproduce the FCI result with errors less than 1×10^{-3} kcal/mol. This demonstrates that ADAPT(m) is able to obtain a quite reasonable reference state even with a very large convergence thresh, such as $\epsilon = 1 \times 10^{-1}$. In addition, increasing m in ADAPT(m) is, in principle, equivalent to sample the Hamiltonian in the linear response space as done in ADAPT(m)/QSE if the same operator pool and parameter space are used. Therefore, it is able to conjecture that ADAPT(m)/QSE significantly improve the accuracy of ADAPT(m), because the QSE wave function is optimized in the complex parameter space.

Although the mean error of 1.30 kcal/mol in ADAPT(3)-SD/QSE is slightly beyond the chemical accuracy, this is almost 3−4 magnitude larger than MEs of ADAPT(m)/QSE. Since the Hamiltonian matrix elements of ADAPT(3)-SD/QSE and ADAPT(m)/QSE are sampled in the same linear-response space with general one- and two-body operators, it reveals that the reference state prepared with ADAPT(3)-SD is even less accurate than ADAPT(1), while the number of parameters in both ADAPT(3)-SD and ADAPT(1) is 30. For QSE-SD, the Hamiltonian is sampled in a much smaller linear response space of dimension being 153 (625 for QSE). This leads to a remarkable deviation of the potential energy curve for ADAPT(3)-SD/QSE-SD with the ME of 3.75 kcal/mol. Therefore, the inclusion of general one- and two-body operators is necessary in the definition of a stable and accurate wave function ansatz.

With the substantial success of the VQE algorithm in simulating ground-state properties, there is a broad interest in applying it to study excited states. For the 1D hydrogen chain, the potential energy surface of different electronic states is important to understand the rich and fascinating phase diagram in quantum material physics. In Figure 3, we present the first excited-state energy and the absolute energy error of the 1D hydrogen chain as a function of R(H−H). The ground-state wave function is obtained with ADAPT(m) or ADAPT-(m)-SD, and the first excited state is computed with the QSE approach. Regardless of the convergence thresh ϵ used in ground-state ADAPT(m) calculations, we obtain exactly the same curves as FCI. For ADAPT(m), mean errors of the first excited-state energy are 5.91×10^{-4}, 5.05×10^{-4}, and 2.04×10^{-4} kcal/mol for $\epsilon = 10^{-1}$, $\epsilon = 10^{-2}$, and $\epsilon = 10^{-3}$, respectively. The performance of ADAPT(3)-SD/QSE in excited-state calculations is quite similar to that in the ground-state calculation. Although the absolute energy error of ADAPT(3)-SD/QSE is acceptable, we recommend to prepare the ground state with ADAPT(m) since it has been validated to be more robust and accurate.

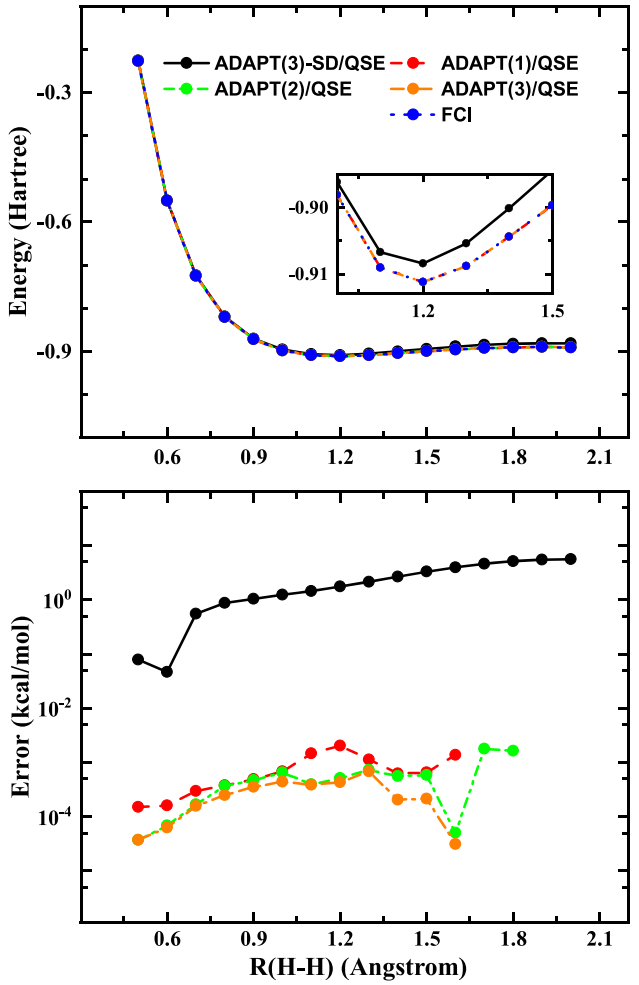

Figure 3. First excited-state potential energy curve and the absolute energy error of the 1D hydrogen chain computed with ADAPT-VQE/QSE. Vanishing points indicate zero error when the energies are recorded with eight decimal places in Hartree.

4. CONCLUSIONS

In this work, we generalize the variational quantum eigenvalue algorithm for periodic systems. We first carry out classical VQE simulations of the 1D infinite hydrogen chain with UCC and ADAPT ansatzes using HF orbitals at sampling *k*-points. UCCSD-VQE and ADAPT(3)-SD totally fail to accurately describe the potential energy surface of the 1D hydrogen chain. The absolute energy error of UCCGSD and ADAPT(3) is acceptable, while it is at least 1−2 magnitude larger than that in the molecular simulation. The detailed analysis of residual error of ACSE reveals that the significant deviation of the energy results from the complex wave function and Hamiltonian generated based on HF orbitals at sampling *k*-points.

Then, we present two schemes to overcome this problem in the VQE algorithm for periodic systems. One is the VQE-K2G approach, which avoids the complex wave function and Hamiltonian involved in VQE through a unitary transforming of HF orbitals at sampling *k*-points in a unit cell into real orbitals at the Γ-point in a supercell. The VQE-K2G algorithm totally removes the residual error of the imaginary part of

https://dx.doi.org/10.1021/acs.jctc.0c00881
J. Chem. Theory Comput. 2020, 16, 6904−6914

ACSE and then achieves the same accuracy as the VQE algorithm in molecular simulations. Another scheme is the combination of VQE with the quantum subspace expansion approach, which offers a better estimation of the energy over the reference state. The VQE/QSE approach projects the Hamiltonian onto the linear response space of the reference state prepared with the VQE algorithm. This can be considered as a *Post* procedure of the VQE correction to the reference state energy. Numerical simulations demonstrate that both the VQE-K2G and VQE/QSE approaches provide an accurate enough description of the potential energy surface of the 1D hydrogen chain. In addition, the accuracy of the VQE/QSE approach is 1−2 magnitude smaller than that of the VQE-K2G approach at the expense of steeply increasing measurements.

In this work, we come to the same conclusion that UCCGSD is more stable than UCCSD as stated in previous studies. The accuracy of UCCGSD without Trotterization is comparable to ADAPT. As Trotterization is introduced in UCC, the wave function expression of eq 17 is quite similar to that in ADAPT as shown in eq 18. However, UCCGSD uses the same coefficients of excitation operators in each Trotterization step, while ADAPT uses difference coefficients. Therefore, ADAPT is expected to be more flexible than UCCGSD with Trotterization. In addition, ADAPT generates an optimized sequence of unitary transformation in eq 18, which is proven to be necessary to find the lowest energy.[58] However, at the beginning of each iteration, ADAPT-VQE needs to compute the gradients in eq 21 at the expense of N_b^8 measurements where N_b is the number of basis functions. Further work should be devoted to reduce the number of measurements.

Finally, we note that the wave function ansatz based on Gaussian basis functions offers a well established solution of electronic structure problems, while a large Gaussian basis set is often required to obtain the converged result. In order to accurately simulate electron structure properties in material science, an alternative approach is to use the Wannier basis function[44] or adaptive local basis function in a discontinuous Galerkin framework,[72] which can reach the complete basis set limit with much fewer basis functions.

APPENDIX: K2G TRANSFORMATION

A simple k-point sampling algorithm proposed by Monkhorst and Pack is used

$$\mathbf{k} = \sum_{i=1}^{3} \frac{2k_i - N_i - 1}{2N_i}\mathbf{b}_i \tag{43}$$

where $k_i = 1, 2, ..., N_i$, and $[N_1, N_2, N_3]$ is the k point used. ($\mathbf{b}_1$, $\mathbf{b}_2$, $\mathbf{b}_3$) are the primitive reciprocal vectors in a unit cell. In this work, we shift Monkhorst-pack grids to include Gamma-point $[0, 0, 0]$ as

$$\mathbf{k} = \sum_{i=1}^{3} \frac{k_i - 1}{N_i}\mathbf{G}_i \tag{44}$$

Given the unit cell with primitive translation vectors ($\mathbf{a}_1$, $\mathbf{a}_2$, $\mathbf{a}_3$), the translation vectors in eq 1 are expressed as

$$\mathbf{R}_n = n_1\mathbf{a}_1 + n_2\mathbf{a}_2 + n_3\mathbf{a}_3 \tag{45}$$

Bloch Hartree−Fock orbitals are rewritten as

$$\begin{aligned}\phi_{p\mathbf{k}}(\mathbf{r}) &= \frac{1}{\sqrt{N}}\sum_{\mu,n} C_{\mu p}(\mathbf{k}) e^{i\mathbf{k}\cdot\mathbf{R}_n}\chi_\mu(\mathbf{r} - \mathbf{R}_n) \\ &= \frac{1}{\sqrt{N}}\sum_{\tilde{\mu},n} C_{\tilde{\mu} p}(\mathbf{k}) e^{i\mathbf{k}\cdot\tilde{\mathbf{R}}_n}\chi_{\tilde{\mu}}(\mathbf{r} - \tilde{\mathbf{R}}_n) \\ &= \frac{1}{\sqrt{N}}\sum_{\tilde{\mu},n} C_{\tilde{\mu} p}(\mathbf{k})\chi_{\tilde{\mu}}(\mathbf{r} - \tilde{\mathbf{R}}_n)\end{aligned} \tag{46}$$

where $\tilde{\mathbf{R}}_n$ is supercell translation vectors

$$\tilde{\mathbf{R}}_n = n_1(N_1\mathbf{a}_1) + n_2(N_2\mathbf{a}_2) + n_3(N_3\mathbf{a}_3) \tag{47}$$

which satisfy $\mathbf{k}\cdot\tilde{R}_n = 2(k_1 + k_2 + k_3 - 3)\pi$. Here, the corresponding supercell is defined with translation vectors ($N_1\mathbf{a}_1$, $N_2\mathbf{a}_2$, $N_3\mathbf{a}_3$).

The Hamiltonian can be expressed with the Hartree−Fock orbitals at sampling k-points as

$$\hat{H}_{HF} = \sum_{p\mathbf{k}} \varepsilon_{p\mathbf{k}} |\phi_{p\mathbf{k}}\rangle\langle\phi_{p\mathbf{k}}| \tag{48}$$

where $\varepsilon_{p\mathbf{k}}$ is the Hartree−Fock orbital energy. The Hartree−Fock eigenvalue equation is

$$\hat{H}_{HF}\phi_{\tilde{p}} = \varepsilon_{\tilde{p}}\phi_{\tilde{p}} \tag{49}$$

which can be expanded in the supercell atomic orbital $\{\chi_{\tilde{\mu}}\}$ representation as

$$\sum_{\tilde{\nu}} F^{sc}_{\tilde{\mu}\tilde{\nu}} C_{\tilde{\nu} p} = \varepsilon_{\tilde{p}} \sum_{\tilde{\nu}} S_{\tilde{\mu}\tilde{\nu}} C_{\tilde{\nu} p} \tag{50}$$

The supercell Fock matrix is

$$\begin{aligned}F^{sc}_{\tilde{\mu}\tilde{\nu}} &= \langle\chi_{\tilde{\mu}}|\hat{H}_{HF}|\chi_{\tilde{\nu}}\rangle \\ &= \sum_{\tilde{\lambda}\tilde{\kappa}} \mathbf{S}^{sc}_{\tilde{\mu}\tilde{\lambda}}(\mathbf{CFC}^{\dagger})_{\tilde{\lambda}\tilde{\kappa}}\mathbf{S}^{sc}_{\tilde{\kappa}\tilde{\nu}}\end{aligned} \tag{51}$$

where

$$F_{\tilde{p}\tilde{q}} = F_{pp}(\mathbf{k})\delta_{\tilde{p}\tilde{q}} = \varepsilon_{p\mathbf{k}}\delta_{\tilde{p}\tilde{q}} \tag{52}$$

AUTHOR INFORMATION

Corresponding Authors

Zhenyu Li − *Hefei National Laboratory for Physical Sciences at the Microscale, University of Science and Technology of China, Hefei, Anhui 230026, China;* orcid.org/0000-0003-2112-9834; Email: zyli@ustc.edu.cn

Jinlong Yang − *Hefei National Laboratory for Physical Sciences at the Microscale, Department of Chemical Physics, and Synergetic Innovation Center of Quantum Information and Quantum Physics, University of Science and Technology of China, Hefei, Anhui 230026, China;* orcid.org/0000-0002-5651-5340; Email: jlyang@ustc.edu.cn

Authors

Jie Liu − *Hefei National Laboratory for Physical Sciences at the Microscale, University of Science and Technology of China, Hefei, Anhui 230026, China;* orcid.org/0000-0002-8140-9144

Lingyun Wan − *Hefei National Laboratory for Physical Sciences at the Microscale, University of Science and Technology of China, Hefei, Anhui 230026, China*

Complete contact information is available at:

https://dx.doi.org/10.1021/acs.jctc.0c00881
J. Chem. Theory Comput. 2020, 16, 6904−6914

https://pubs.acs.org/10.1021/acs.jctc.0c00881

Notes

The authors declare no competing financial interest.

■ ACKNOWLEDGMENTS

This work is supported by the National Natural Science Foundation of China (21688102, 21825302, 21803065), by the National Key Research and Development Program of China (2016YF A0200604), and Anhui Initiative in Quantum Information Technologies (AHY090400).

■ REFERENCES

(1) Cohen, A. J.; Mori-Sanchez, P.; Yang, W. Insights into current limitations of density functional theory. *Science* **2008**, *321*, 792−794.
(2) Zhao, Y.; Truhlar, D. G. Density functionals with broad applicability in chemistry. *Acc. Chem. Res.* **2008**, *41*, 157−167.
(3) Cohen, A. J.; Mori-Sanchez, P.; Yang, W. Challenges for density functional theory. *Chem. Rev.* **2012**, *112*, 289−320.
(4) Sun, J.; Bartlett, R. J. Second-order many-body perturbation-theory calculations in extended systems. *J. Chem. Phys.* **1996**, *104*, 8553−8565.
(5) Ayala, P. Y.; Kudin, K. N.; Scuseria, G. E. Atomic orbital Laplace-transformed second-order Møller-Plesset theory for periodic systems. *J. Chem. Phys.* **2001**, *115*, 9698−9707.
(6) Shukla, A.; Dolg, M.; Fulde, P.; Stoll, H. Wave-function-based correlated ab initio calculations on crystalline solids. *Phys. Rev. B: Condens. Matter Mater. Phys.* **1999**, *60*, 5211−5216.
(7) Gillan, M. J.; Alfè, D.; Gironcoli, S. d.; Manby, F. R. High-precision calculation of Hartree-Fock energy of crystals. *J. Comput. Chem.* **2008**, *29*, 2098−2106.
(8) Nolan, S. J.; Gillan, M. J.; Alfè, D.; Allan, N. L.; Manby, F. R. Calculation of properties of crystalline lithium hydride using correlated wave function theory. *Phys. Rev. B: Condens. Matter Mater. Phys.* **2009**, *80*, 165109.
(9) Booth, G. H.; Grüneis, A.; Kresse, G.; Alavi, A. Towards an exact description of electronic wavefunctions in real solids. *Nature* **2013**, *493*, 365−370.
(10) McClain, J.; Sun, Q.; Chan, G. K.-L.; Berkelbach, T. C. Gaussian-Based Coupled-Cluster Theory for the Ground-State and Band Structure of Solids. *J. Chem. Theory Comput.* **2017**, *13*, 1209−1218.
(11) Hummel, F.; Tsatsoulis, T.; Grüneis, A. Low rank factorization of the Coulomb integrals for periodic coupled cluster theory. *J. Chem. Phys.* **2017**, *146*, 124105.
(12) Riley, K. E.; Pitoňák, M.; Jurečka, P.; Hobza, P. Stabilization and Structure Calculations for Noncovalent Interactions in Extended Molecular Systems Based on Wave Function and Density Functional Theories. *Chem. Rev.* **2010**, *110*, 5023−5063.
(13) Bravyi, S. B.; Kitaev, A. Y. Fermionic Quantum Computation. *Ann. Phys.* **2002**, *298*, 210−226.
(14) Georgescu, I. M.; Ashhab, S.; Nori, F. Quantum simulation. *Rev. Mod. Phys.* **2014**, *86*, 153−185.
(15) Preskill, J. Quantum Computing in the NISQ era and beyond. *Quantum* **2018**, *2*, 79.
(16) Cao, Y.; Romero, J.; Olson, J. P.; Degroote, M.; Johnson, P. D.; Kieferová, M.; Kivlichan, I. D.; Menke, T.; Peropadre, B.; Sawaya, N. P. D.; Sim, S.; Veis, L.; Aspuru-Guzik, A. Quantum Chemistry in the Age of Quantum Computing. *Chem. Rev.* **2019**, *119*, 10856−10915.
(17) McArdle, S.; Endo, S.; Aspuru-Guzik, A.; Benjamin, S. C.; Yuan, X. Quantum computational chemistry. *Rev. Mod. Phys.* **2020**, *92*, 015003.
(18) Du, J.; Xu, N.; Peng, X.; Wang, P.; Wu, S.; Lu, D. NMR Implementation of a Molecular Hydrogen Quantum Simulation with Adiabatic State Preparation. *Phys. Rev. Lett.* **2010**, *104*, 030502.
(19) Peruzzo, A.; McClean, J.; Shadbolt, P.; Yung, M.-H.; Zhou, X.-Q.; Love, P. J.; Aspuru-Guzik, A.; O' Brien, J. L. A variational eigenvalue solver on a photonic quantum processor. *Nat. Commun.* **2014**, *5*, 4213.
(20) Wecker, D.; Hastings, M. B.; Troyer, M. Progress towards practical quantum variational algorithms. *Phys. Rev. A: At., Mol., Opt. Phys.* **2015**, *92*, 042303.
(21) O' Malley, P. J. J.; Babbush, R.; Kivlichan, I. D.; Romero, J.; McClean, J. R.; Barends, R.; Kelly, J.; Roushan, P.; Tranter, A.; Ding, N.; Campbell, B.; Chen, Y.; Chen, Z.; Chiaro, B.; Dunsworth, A.; Fowler, A. G.; Jeffrey, E.; Lucero, E.; Megrant, A.; Mutus, J. Y.; Neeley, M.; Neill, C.; Quintana, C.; Sank, D.; Vainsencher, A.; Wenner, J.; White, T. C.; Coveney, P. V.; Love, P. J.; Neven, H.; Aspuru-Guzik, A.; Martinis, J. M. Scalable Quantum Simulation of Molecular Energies. *Phys. Rev. X* **2016**, *6*, 031007.
(22) Harrow, A. W.; Montanaro, A. Quantum computational supremacy. *Nature* **2017**, *549*, 203.
(23) Reiher, M.; Wiebe, N.; Svore, K. M.; Wecker, D.; Troyer, M. Elucidating reaction mechanisms on quantum computers. *Proc. Natl. Acad. Sci. U. S. A.* **2017**, *114*, 7555.
(24) Kandala, A.; Mezzacapo, A.; Temme, K.; Takita, M.; Brink, M.; Chow, J. M.; Gambetta, J. M. Hardware-efficient variational quantum eigensolver for small molecules and quantum magnets. *Nature* **2017**, *549*, 242.
(25) Hempel, C.; Maier, C.; Romero, J.; McClean, J.; Monz, T.; Shen, H.; Jurcevic, P.; Lanyon, B. P.; Love, P.; Babbush, R.; Aspuru-Guzik, A.; Blatt, R.; Roos, C. F. Quantum Chemistry Calculations on a Trapped-Ion Quantum Simulator. *Phys. Rev. X* **2018**, *8*, 031022.
(26) Santagati, R.; Wang, J.; Gentile, A. A.; Paesani, S.; Wiebe, N.; McClean, J. R.; MorleyShort, S.; Shadbolt, P. J.; Bonneau, D.; Silverstone, J. W.; Tew, D. P.; Zhou, X.; O' Brien, J. L.; Thompson, M. G. Witnessing eigenstates for quantum simulation of Hamiltonian spectra. *Sci. Adv.* **2018**, *4*, eaap9646.
(27) Grimsley, H. R.; Economou, S. E.; Barnes, E.; Mayhall, N. J. An adaptive variational algorithm for exact molecular simulations on a quantum computer. *Nat. Commun.* **2019**, *10*, 3007.
(28) Colless, J. I.; Ramasesh, V. V.; Dahlen, D.; Blok, M. S.; Kimchi-Schwartz, M. E.; McClean, J. R.; Carter, J.; de Jong, W. A.; Siddiqi, I. Computation of Molecular Spectra on a Quantum Processor with an Error-Resilient Algorithm. *Phys. Rev. X* **2018**, *8*, 011021.
(29) Babbush, R.; Wiebe, N.; McClean, J.; McClain, J.; Neven, H.; Chan, G. K.-L. Low-Depth Quantum Simulation of Materials. *Phys. Rev. X* **2018**, *8*, 011044.
(30) Kivlichan, I. D.; McClean, J.; Wiebe, N.; Gidney, C.; Aspuru-Guzik, A.; Chan, G. K.-L.; Babbush, R. Quantum Simulation of Electronic Structure with Linear Depth and Connectivity. *Phys. Rev. Lett.* **2018**, *120*, 110501.
(31) Kivlichan, I. D.; Gidney, C.; Berry, D. W.; Wiebe, N.; McClean, J.; Sun, W.; Jiang, Z.; Rubin, N.; Fowler, A.; Aspuru-Guzik, A.; Neven, H.; Babbush, R. Improved Fault-Tolerant Quantum Simulation of Condensed-Phase Correlated Electrons via Trotterization. *Quantum* **2020**, *4*, 296.
(32) Childs, A. M.; Su, Y. Nearly Optimal Lattice Simulation by Product Formulas. *Phys. Rev. Lett.* **2019**, *123*, 050503.
(33) Haah, J.; Hastings, M. B.; Kothari, R.; Low, G. H. Quantum algorithm for simulating real time evolution of lattice Hamiltonians. arXiv:quant-ph, 2018, *arXiv:1801.03922*. https://arxiv.org/abs/1801.03922 (accessed 2020-10-13).
(34) Aspuru-Guzik, A.; Dutoi, A. D.; Love, P. J.; Head-Gordon, M. Simulated Quantum Computation of Molecular Energies. *Science* **2005**, *309*, 1704.
(35) Whitfield, J. D.; Biamonte, J.; Aspuru-Guzik, A. Simulation of electronic structure Hamiltonians using quantum computers. *Mol. Phys.* **2011**, *109*, 735−750.
(36) McClean, J. R.; Romero, J.; Babbush, R.; Aspuru-Guzik, A. The theory of variational hybrid quantum-classical algorithms. *New J. Phys.* **2016**, *18*, 023023.
(37) McClean, J. R.; Kimchi-Schwartz, M. E.; Carter, J.; de Jong, W. A. Hybrid quantum-classical hierarchy for mitigation of decoherence and determination of excited states. *Phys. Rev. A: At., Mol., Opt. Phys.* **2017**, *95*, 042308.

https://dx.doi.org/10.1021/acs.jctc.0c00881
J. Chem. Theory Comput. 2020, 16, 6904−6914

(38) Romero, J.; Babbush, R.; McClean, J. R.; Hempel, C.; Love, P. J.; Aspuru-Guzik, A. Strategies for quantum computing molecular energies using the unitary coupled cluster ansatz. *Quantum Sci. Technol.* **2019**, *4*, 014008.
(39) Evangelista, F. A. Alternative single-reference coupled cluster approaches for multireference problems: the simpler, the better. *J. Chem. Phys.* **2011**, *134*, 224102.
(40) VandeVondele, J.; Krack, M.; Mohamed, F.; Parrinello, M.; Chassaing, T.; Hutter, J. Quickstep: Fast and accurate density functional calculations using a mixed Gaussian and plane waves approach. *Comput. Phys. Commun.* **2005**, *167*, 103.
(41) Kleinman, L.; Bylander, D. M. Efficacious Form for Model Pseudopotentials. *Phys. Rev. Lett.* **1982**, *48*, 1425−1428.
(42) Goedecker, S.; Teter, M.; Hutter, J. Separable dual-space Gaussian pseudopotentials. *Phys. Rev. B: Condens. Matter Mater. Phys.* **1996**, *54*, 1703.
(43) Hartwigsen, C.; Goedecker, S.; Hutter, J. Relativistic separable dual-space Gaussian pseudopotentials from H to Rn. *Phys. Rev. B: Condens. Matter Mater. Phys.* **1998**, *58*, 3641.
(44) Marzari, N.; Mostofi, A. A.; Yates, J. R.; Souza, I.; Vanderbilt, D. Maximally localized Wannier functions: Theory and applications. *Rev. Mod. Phys.* **2012**, *84*, 1419−1475.
(45) Nooijen, M. Can the Eigenstates of a Many-Body Hamiltonian Be Represented Exactly Using a General Two-Body Cluster Expansion? *Phys. Rev. Lett.* **2000**, *84*, 2108.
(46) Mukherjee, D.; Kutzelnigg, W. Some comments on the coupled cluster with generalized singles and doubles (CCGSD) ansatz. *Chem. Phys. Lett.* **2004**, *397*, 174.
(47) Kutzelnigg, W. Quantum chemistry in Fock space. I. The universal wave and energy operators. *J. Chem. Phys.* **1982**, *77*, 3081.
(48) Bartlett, R. J.; Kucharski, S. A.; Noga, J. Alternative coupled-cluster ansätze II. The unitary coupled-cluster method. *Chem. Phys. Lett.* **1989**, *155*, 133.
(49) Taube, A. G.; Bartlett, R. J. New perspectives on unitary coupled-cluster theory. *Int. J. Quantum Chem.* **2006**, *106*, 3393.
(50) Harsha, G.; Shiozaki, T.; Scuseria, G. E. On the difference between variational and unitary coupled cluster theories. *J. Chem. Phys.* **2018**, *148*, 044107.
(51) Ronen, S. Can the Eigenstates of a Many-Body Hamiltonian Be Represented Exactly Using a General Two-Body Cluster Expansion? *Phys. Rev. Lett.* **2003**, *91*, 123002.
(52) Mazziotti, D. A. Exactness of wave functions from two-body exponential transformations in many-body quantum theory. *Phys. Rev. A: At., Mol., Opt. Phys.* **2004**, *69*, 012507.
(53) Nakatsuji, H. Scaled Schrödinger Equation and the Exact Wave Function. *Phys. Rev. Lett.* **2004**, *93*, 030403.
(54) Shen, Y.; Zhang, X.; Zhang, S.; Zhang, J.-N.; Yung, M.-H.; Kim, K. Quantum implementation of the unitary coupled cluster for simulating molecular electronic structure. *Phys. Rev. A: At., Mol., Opt. Phys.* **2017**, *95*, 020501.
(55) Lee, J.; Huggins, W. J.; Head-Gordon, M.; Whaley, K. B. Generalized Unitary Coupled Cluster Wave functions for Quantum Computation. *J. Chem. Theory Comput.* **2019**, *15*, 311−324.
(56) Poulin, D.; Hastings, M. B.; Wecker, D.; Wiebe, N.; Doberty, A. C.; Troyer, M. The Trotter Step Size Required for Accurate Quantum Simulation of Quantum Chemistry. *Quantum Inf. Comput.* **2015**, *15*, 361.
(57) Babbush, R.; McClean, J.; Wecker, D.; Aspuru-Guzik, A.; Wiebe, N. Chemical basis of Trotter-Suzuki errors in quantum chemistry simulation. *Phys. Rev. A: At., Mol., Opt. Phys.* **2015**, *91*, 022311.
(58) Grimsley, H. R.; Claudino, D.; Economou, S. E.; Barnes, E.; Mayhall, N. J. Is the Trotterized UCCSD Ansatz Chemically Well-Defined? *J. Chem. Theory Comput.* **2020**, *16*, 1−6.
(59) Piecuch, P.; Kowalski, K.; Fan, P.-D.; Jedziniak, K. Exactness of Two-Body Cluster Expansions in Many-Body Quantum Theory. *Phys. Rev. Lett.* **2003**, *90*, 113001.
(60) Davidson, E. R. Exactness of the General Two-Body Cluster Expansion in Many-Body Quantum Theory. *Phys. Rev. Lett.* **2003**, *91*, 123001.
(61) Mazziotti, D. A. Quantum Chemistry without Wave Functions: Two-Electron Reduced Density Matrices. *Acc. Chem. Res.* **2006**, *39*, 207−215.
(62) Mazziotti, D. A. Anti-Hermitian part of the contracted Schrödinger equation for the direct calculation of two-electron reduced density matrices. *Phys. Rev. A: At., Mol., Opt. Phys.* **2007**, *75*, 022505.
(63) Ollitrault, P. J.; Kandala, A.; Chen, C.-F.; Barkoutsos, P. K.; Mezzacapo, A.; Pistoia, M.; Sheldon, S.; Woerner, S.; Gambetta, J.; Tavernelli, I. Quantum equation of motion for computing molecular excitation energies on a noisy quantum processor. arXiv:quant-ph, 2019, *arXiv:1910.12890*. https://arxiv.org/abs/1910.12890 (accessed 2020-10-13).
(64) ADAPT-VQE. https://github.com/mayhallgroup/adapt-vqe (accessed 2020-10-13).
(65) McClean, J. R.; Sung, K. J.; Kivlichan, I. D.; Cao, Y.; Dai, C.; Fried, E. S.; Gidney, C.; Gimby, B.; Gokhale, P.; Häner, T.; Hardikar, T.; Havlíček, V.; Higgott, O.; Huang, C.; Izaac, J.; Jiang, Z.; Liu, X.; McArdle, S.; Neeley, M.; O'Brien, T.; O'Gorman, B.; Ozfidan, I.; Radin, M. D.; Romero, J.; Rubin, N.; Sawaya, N. P. D.; Setia, K.; Sim, S.; Steiger, D. S.; Steudtner, M.; Sun, Q.; Sun, W.; Wang, D.; Zhang, F.; Babbush, R. *OpenFermion: The Electronic Structure Package for Quantum Computers*. arXiv:quant-ph, 2017, *arXiv:1710.07629*. https://arxiv.org/abs/1710.07629 (accessed 2020-10-13).
(66) Sun, Q.; Berkelbach, T. C.; Blunt, N. S.; Booth, G. H.; Guo, S.; Li, Z.; Liu, J.; McClain, J. D.; Sayfutyarova, E. R.; Sharma, S.; Wouters, S.; Chan, G. K.-L. PySCF: the Python-based simulations of chemistry framework. *Wiley Interdiscip. Rev.: Comput. Mol. Sci.* **2018**, *8*, e1340.
(67) Virtanen, P.; Gommers, R.; Oliphant, T. E.; Haberland, M.; Reddy, T.; Cournapeau, D.; Burovski, E.; Peterson, P.; Weckesser, W.; Bright, J.; van der Walt, S. J.; Brett, M.; Wilson, J.; Jarrod Millman, K.; Mayorov, N.; Nelson, A. R. J.; Jones, E.; Kern, R.; Larson, E.; Carey, C.; Polat, İ.; Feng, Y.; Moore, E. W.; Vand erPlas, J.; Laxalde, D.; Perktold, J.; Cimrman, R.; Henriksen, I.; Quintero, E. A.; Harris, C. R.; Archibald, A. M.; Ribeiro, A. H.; Pedregosa, F.; van Mulbregt, P.; Contributors, S. SciPy 1.0: Fundamental Algorithms for Scientific Computing in Python. *Nat. Methods* **2020**, *17*, 261−272.
(68) Welden, A. R.; Rusakov, A. A.; Zgid, D. Exploring connections between statistical mechanics and Green's functions for realistic systems: Temperature dependent electronic entropy and internal energy from a self-consistent second-order Green's function. *J. Chem. Phys.* **2016**, *145*, 204106.
(69) Rusakov, A. A.; Zgid, D. Self-consistent second-order Green's function perturbation theory for periodic systems. *J. Chem. Phys.* **2016**, *144*, 054106.
(70) Motta, M.; Genovese, C.; Ma, F.; Cui, Z.-H.; Sawaya, R.; Chan, G. K.-L.; Chepiga, N.; Helms, P.; Jimenez-Hoyos, C.; Millis, A. J.; Ray, U.; Ronca, E.; Shi, H.; Sorella, S.; Stoudenmire, E. M.; White, S. R.; Zhang, S. *Ground-state properties of the hydrogen chain: insulator-to-metal transition, dimerization, and magnetic phases*. arXiv:cond-mat.str-el, 2019, *arXiv:1911.01618*.https://arxiv.org/abs/1911.01618 (accessed 2020-10-13).
(71) Liu, Y.; Shen, T.; Zhang, H.; Rubenstein, B. Unveiling the Finite Temperature Physics of Hydrogen Chains via Auxiliary Field Quantum Monte Carlo. *J. Chem. Theory Comput.* **2020**, *16*, 4298−4314.
(72) Zhang, G.; Lin, L.; Hu, W.; Yang, C.; Pask, J. E. Adaptive local basis set for Kohn-Sham density functional theory in a discontinuous Galerkin framework II: Force, vibration, and molecular dynamics calculations. *J. Comput. Phys.* **2017**, *335*, 426−443.

https://dx.doi.org/10.1021/acs.jctc.0c00881
J. Chem. Theory Comput. 2020, 16, 6904−6914